ORNL/CP-101022

# An Anticipatory Model of Cavitation

To be presented at the
Applications and Science of Computational Intelligence II Conference

Sponsored by
SPIE—The International Society for Optical Engineering

April 6, 1999
Orlando, Florida



Authors:
Stephen W. Kercel
Glenn O. Allgood
William B. Dress Jr.
James O. Hylton

Oak Ridge National Laboratory*
P.O. Box 2008
Oak Ridge, TN 37831-6011



* Managed and Operated by Lockheed Martin Energy Research Corporation for the U.S. Department of Energy under Contract DE-AC05-96OR22464

# An anticipatory model of cavitation

Stephen W. Kercel,* Glenn O. Allgood, William B. Dress, James O. Hylton

Oak Ridge National Laboratory,+ P.O. Box 2008, MS-6011, Oak Ridge, TN 37831-6011

## ABSTRACT

The Anticipatory System (AS) formalism developed by Robert Rosen provides some insight into the problem of embedding intelligent behavior in machines. AS emulates the anticipatory behavior of biological systems. AS bases its behavior on its expectations about the near future and those expectations are modified as the system gains experience. The expectation is based on an internal model that is drawn from an appeal to physical reality. To be adaptive, the model must be able to update itself. To be practical, the model must run faster than real-time. The need for a physical model and the requirement that the model execute at extreme speeds, has held back the application of AS to practical problems.

Two recent advances make it possible to consider the use of AS for practical intelligent sensors. First, advances in transducer technology make it possible to obtain previously unavailable data from which a model can be derived. For example, acoustic emissions (AE) can be fed into a Bayesian system identifier that enables the separation of a weak characterizing signal, such as the signature of pump cavitation precursors, from a strong masking signal, such as a pump vibration feature. The second advance is the development of extremely fast, but inexpensive, digital signal processing hardware on which it is possible to run an adaptive Bayesian-derived model faster than real-time. This paper reports the investigation of an AS using a model of cavitation based on hydrodynamic principles and Bayesian analysis of data from high-performance AE sensors.

**Keywords:** anticipatory system, Bayesian, machine intelligence, model-based, cavitation

## 1. INTRODUCTION

The objective of this research was to find a reliable signature of cavitation and its precursors in flowing fluids. There are two reasons why this is valuable. First, cavitation is a widely occurring undesirable operating condition that can cause irreversible damage in fluid-handling systems, such as pumps. It occurs abruptly and its onset is not predictable by conventional methods. Second, to keep cavitation from occurring, pumps are operated conservatively far from the point of cavitation inception, resulting in a loss of process efficiency. Nevertheless, cavitation could be easily controllable by manipulating the pump inlet and outlet pressures if a reliable signal warning of impending or incipient cavitation were available. Such a scheme would enable a pump to operate at high efficiency while avoiding cavitation altogether.

This cannot effectively be done by conventional methods. As a consequence of evolving effects, such as wear, among the pump properties that change over time is the point at which cavitation begins to occur. Thus, it is not practical to make a one-time or occasional observation of the point of cavitation inception and then assume that it will remain fixed. What must be observed is a feature that indicates, in real-time, that *cavitation is about to occur.*

Although cavitation is a catastrophic effect, the physics of cavitation is reasonably well understood. A nonlinear model of the fluid dynamics that includes extractable parameters of the acoustic emission (AE) signature and describes the onset of cavitation should be readily constructible. Thus, cavitation is an ideal effect for demonstrating the utility of a model-based Anticipatory System (AS). Since the location of the point of bifurcation into catastrophe is context dependent, cavitation is not reliably predictable by conventional models. However, it is well understood and we should be able to construct the anticipatory model from experimental data and the existing physics.

* Correspondence: Email: kercelsw@ornl.gov; Telephone: 423-574-5278; Fax: 423-574-6663

+ Managed and Operated by Lockheed Martin Energy Research Corporation for the U.S. Department of Energy under Contract DE-AC05-96OR22464

## 2. CAVITATION

Cavitation is the formation of vapor bubbles in a liquid whose local pressure falls below the vaporization point for the ambient temperature of the liquid. It is complementary to the idea of boiling, in which the local temperature rises above the vaporization point for the ambient pressure of the liquid. Cavitation is a problem for several reasons. As with boiling, it is turbulent and disrupts attempts to control flows. Also, when the vapor bubbles recondense to liquid, the bubbles collapse violently, creating damaging shock waves in the liquid.

The cavitation bubble starts its growth from a nucleation site. The bubble forms when the nucleation site in a flowing liquid passes into a local region of low pressure. Seldom are fluids pure single-phase liquids. The nucleation site might be a microscopic particle of contamination or a microscopic bubble of the fluid vapor. The fluid usually contains many nucleation sites with a wide distribution of sizes.

If cavitation simply started whenever the minimum pressure, p, in a liquid flow dropped below the vapor pressure, $p_v$, of the flowing liquid, then the prediction of the inception of cavitation would be straightforward. However, many physical effects cause the actual inception point to be far from that predicted by this criterion. One of the most troublesome is the effect of surface tension at a nucleation site. Since the liquid can withstand tensions below the vapor pressure, this has to be taken into account. A microbubble of radius, $R_N$, and surface tension, $S$, containing only vapor, is in equilibrium if the liquid pressure is $p = p_V - 2S/R_N$. The liquid pressure must fall below this critical point for cavitation to start. Unfortunately, the liquid contains a great many nucleation sites having a great many radii. These vary with the physical situation and with the quality of the fluid.[1] Therefore, the onset of cavitation and its precursors must be observed directly.

Air can cause cavitation. Dissolved air will contribute to the partial pressure of the cavitation bubble. As the bubble moves to a region of higher pressure, the vaporized liquid recondenses and leaves an air bubble remaining. Air is slow to redissolve.[1] Thus, one of the things that can go wrong with a cavitation experiment in a test loop is that the air bubbles from the first pass are not redissolved in the loop. Therefore, the return leg of the test loop must be long enough and at high enough pressure for the air bubbles to become reabsorbed. Otherwise, the number of nucleation sites will grow rapidly as the experiment runs.

There are several other phenomena that affect bubble formation.[2] The first is residence time. The cavitation bubble takes a finite time to form. Residence time depends on pump size, flow rate, and temperature; if the cavitation nucleus is in the region of low pressure for less than the residence time, the bubble will not form. Turbulence causes localized low pressure, significantly below the mean pressure of the flow, and is often the site of incipient cavitation. This effect is dependent on the Reynolds number, but is a separate effect from the dependency of the pressure coefficient on the Reynolds number. Surface roughness also creates localized low-pressure perturbations. Localized low pressure is a departure from the simplifying assumption that the pressure is uniform (at average value) through a cross section of the stream.

Practically everything that can be said about the properties of the cavitation bubble is based on the Rayleigh-Plesset equation (Equation 1).[3] The generalized differential equation gives the instantaneous bubble radius, R(t), in response to the driving pressure far from the bubble, $p_\infty(t)$. The equation is based on a few simplifying assumptions that turn out to be quite reasonable in practice.

The simplifying assumptions include the following. A single spherical bubble is in an infinite liquid domain whose remote temperature, $T_\infty$, is constant in time. There is no uniform heating of the liquid due to radiation or internal heating. Liquid density, $\rho_L$, is assumed constant. Dynamic viscosity, $\mu_L$, is assumed constant and uniform. The bubble contents are homogeneous, and the temperature, $T_B(t)$, and pressure, $p_B(t)$, inside the bubble are independent of location. It is also assumed that the bubble contains a contaminant gas with a partial pressure, $p_{Go}$, (given a reference bubble radius $R_0$, and temperature, $T_\infty$). Finally, it is assumed that there is negligible mass transfer between the liquid and the contaminant gas.

$$\underbrace{\frac{p_v(T_\infty)}{\rho_L}}_{(1)} - \frac{p_\infty(t)}{\rho_L} + \underbrace{\frac{p_v(T_B)}{\rho_L}}_{(2)} - \frac{p_v(T_\infty)}{\rho_L} + \underbrace{\frac{p_{Go}}{\rho_L}\left(\frac{T_B}{T_\infty}\right)}_{(3)}\left(\frac{R_o}{R}\right)^3 = \underbrace{R\frac{d^2R}{dt^2}}_{(4)} + \frac{3}{2}\left(\frac{dR}{dt}\right)^2 + \underbrace{\frac{4\nu_L}{R}\frac{dR}{dt}}_{(5)} + \underbrace{\frac{2S}{\rho_L R}}_{(6)} \tag{1}$$

The equation is best understood by considering its terms. The driving (first) term depends on the pressure in the liquid far from the bubble, $p_\infty(t)$. The remote vapor pressure of the liquid, $p_v T(\infty)$, depends only on the liquid and the remote temperature. The liquid density is a property of the liquid. The second term is the thermal term. If thermal effects are to be neglected, then $T_B(t) = T_\infty$, and $p_v(T_B)-p_v(T_\infty) = 0$. When this term is non-zero, it can greatly affect the growth rate of the bubble. The third term accounts for the effect of the contaminant gas. The fifth term depends on the kinematic viscosity of the liquid, $\nu_L$. The sixth term depends on the surface tension of the liquid, $S$.

A consequence of the Rayleigh-Plesset equation is bubble instability. If the bubble is greater than a critical radius, any small perturbation in pressure will cause it to grow without bound. The critical radius is approximately $4S/3(p_v-p_\infty)$. As the pressure, $p_\infty$, drops, the critical radius drops, which means that more nuclei in a given distribution of nucleation site radii are induced to cavitate. This is why there is a rapid increase in the number of visible bubbles in a cavitating flow as the pressure drops.[4]

In the most simplified case, the solution of the Rayleigh-Plesset equation predicts an oscillating response, in which the contracting part of the bubble oscillation represents a catastrophic collapse. In reality the oscillation does not occur. As the bubble approaches zero radius, it becomes unstable to non-spherical perturbations; it shatters into a cloud of even smaller bubbles during the first collapse. This generates powerful shock waves that produce the AE signature.[5] The cloud will then expand and collapse, and this will also produce powerful shock waves.[6]

The collapse of a bubble near a hard surface produces first a microjet directed toward the hard surface and then the collapsing bubble cloud. Due to its high, local pressure, the microjet emits noise and causes damage. The collapsing remnant bubble cloud causes even more noise and damage than the microjet, although the mechanism by which it does so is not understood.[7]

The natural frequency at which an isolated bubble oscillates in a quiescent liquid can also be determined from the Rayleigh-Plesset equation.[8] For typical liquids in typical pump environments, the natural frequency is predicted to be between 10 kHz and 1 MHz. Acoustic pressure varies as the second derivative of bubble volume.[8]

Kumar and Brennen have determined the second-order nonlinear effects for an isolated bubble.[9] The bubble radius will oscillate at integral harmonics of the excitation if the excitation is a remote pressure oscillating at a single harmonic frequency. Because the response varies inversely with the order of the harmonic, only the first 50 harmonics contribute to the response. For weak excitation, this model tracks fairly well with a direct numerical solution of the equation presented by Kumar. More accurate solutions appear in the literature, but Kumar's is easily extended to bubble clouds.

The AE signature of cavitation noise is broadband and has been subjected to various theoretical and experimental investigations. It is noteworthy that practically all experimental results are reported as a power spectral density derived from a Fourier analysis of the experimental data.[10] There appears to be no report in the literature of the fine details in frequency resolution that could be obtained from Bayesian analysis or the transient details that would emerge from wavelet analysis.

The conventional understanding of the character of the AE signature is as follows. The dominant frequency of the signature is related to the natural frequency of the typical cavitation bubble. This is in turn related to the size of the nucleation site, but there are many nucleation sites throughout a distribution of sizes. There is a critical frequency, f, such that $ft_{TC} = 1$, where $t_{TC} = 0.915R_0[\rho_L/(p_\infty - p_v)]^{1/2}$ is the collapse time of the bubble whose most probable nucleation radius is $R_0$. At the critical frequency, the power spectral density is highest. Well below the critical frequency, the power spectral density increases as $f^4$. Well above the critical frequency, the power spectral density decreases approximately as $1/f^2$. Different researchers have reported different results for the complex behavior near the critical frequency.

It is noteworthy that in a bubbly liquid medium for frequencies above 200 kHz, the attenuation of the pressure wave is about 5 dB/cm, as compared to 25 dB/cm at the average bubble natural frequency of 100 kHz. Thus, even if the higher frequency effects should occur less commonly, they may still be as easy to observe as the low frequency events that start out stronger. Another way to interpret this effect is to note that although most of the energy is generated near the average bubble natural frequency, these bubbles act as absorbers. Energy from the collapse of bubbles far away from the average size is smaller, but since it is not so strongly absorbed, it should be easier to detect.[11]

In a bubbly flow, there is a shock wave. Viscosity will affect the properties of the shock wave and lead to damping effects. For reasonably low void fractions, the shock wave ringing effect occurs at about half the natural frequency of the isolated bubble. In the time domain, at a stationary observation point, the shock wave will be perceived as a rising and then damped nonlinear oscillation. The shock wave contributes to the acoustic signature in cavitating flows.[12]

As cavitation becomes severe, the cavitation bubbles cannot be assumed to act independently of each other—a cloud of interacting bubbles forms.[9] This is a serious concern because the collapse of the bubble cloud causes considerably more damage than the collapse of an isolated bubble. The natural frequency of the bubble cloud is a fraction of the individual bubble.[13] Hence, it is expected that the frequency of AE signatures should drop as cavitation becomes more severe.

Thus, cavitation often occurs as an oscillating, flowing bubble cloud. This will have a number of modes and a number of natural frequencies, all lower than the natural frequency of an isolated bubble. For a small void fraction, all the cloud natural frequencies will be in a narrow range just below the isolated bubble natural frequency. For a large void fraction, the cloud natural frequencies will occupy a large range below the bubble natural frequency. Since damping is strong near the isolated bubble natural frequency and since the outside of the cloud shields the rest of the world from effects inside the cloud, the dominant effect in a cloud in a damping medium is the response at the lowest cloud natural frequency. Thus, the response will be seen as a large peak at the lowest cloud natural frequency and a smaller peak at the bubble natural frequency, with the strength and frequency of the cloud response decreasing with increasing void fraction.[14] This means that the AE signature should exhibit a chirp whose frequency decreases with time.

Note that the foregoing paragraph only describes the linear effects of a bubble cloud in a flow; other effects, at higher frequencies occur when nonlinear effects are taken into account. Harmonic cascading is the effect of harmonics at relatively low frequencies exciting the natural frequencies of smaller bubbles that leads to higher frequency effects. Whereas the linearized analysis of bubble cloud dynamics showed the lowest cloud natural frequency as the dominant effect, nonlinear analysis says that the low-order harmonics of the lowest cloud natural frequency are also strongly present. This can stimulate harmonic cascading if the fluid contains nucleation sites over a range of small sizes.[9]

The summary of the foregoing theory suggests that the AE signature should be most readily detectable in the 100-200 kHz band. Fluid viscosity will cause the signature to be damped. Decreasing natural frequency of the bubble cloud with increasing void-fraction will cause the signature to chirp downward in frequency. As seen in Section 5, this is exactly what the authors have observed experimentally.

## 3. ANTICIPATORY SYSTEMS

Of what use are these signatures? The objective of this research is to develop a system that will anticipate cavitation. The anticipation is based on the recognition of precursor features in non-cavitating fluid. This strategy is similar to the appeal to the "Doggie Existence Theorem" in mine detection.[15] The argument being that if dogs can detect mines, then the problem is solvable. A slight generalization of the "Doggie Existence Theorem" is a common justification for the development of electronic systems that seek to emulate biological cognition. Assuming that biological percepts can be encoded, an electronic system should be able to emulate the process by which a biological system extracts features from sensory cues to identify the presence of a suspected effect.

Does the idea of computational emulation of a biological process actually provide a practical basis for a novel approach to extracting meaning from noisy data? Recent research by Landauer and Bellman suggests that, in principle it does.[16] Biological systems process signs and symbols to gain awareness of their environment and their processing skill improves with experience. They commonly use the data inferred from these symbols to perform classification and grouping and *they do not do so by identifying boundaries between classes*. The way that biological systems perform classification suggests that there exists a semiotic unifying principle of classification that is applicable to computational systems.[17]

Landauer and Bellman define semiotics as "the study of the appearance (visual or otherwise), meaning, and use of symbols and symbol systems." From their examination of classification by biological systems, they conclude that it would require a radical shift in how symbols are represented in computers to emulate the biological classification process in hardware. However, they argue that semiotic theory should provide the theoretical basis for just such a radical shift. Landauer and Bellman do not claim to have discovered the unifying semiotic principle of pattern-recognition but they suggest that it must be inductive in character.[18]

Indeed, the development of a unified inductive-learning model is the key to artificial intelligence.[19,20] Induction is defined as a mode of reasoning that increases the information content of a given body of data. The application to pattern-recognition in general is obvious. An inductive pattern recognizer would learn the common characterizing attributes of all (possibly infinitely many) members of a class from observation of a finite (preferably small) set of samples from the class and a finite set of samples not from the class. The problem arises due to the fact that none of the commonly used "learning" paradigms (neural nets, nearest neighbor algorithms, etc.) are actually capable of performing induction.

How then should this induction be performed? The leading thinkers in machine intelligence believe it should somehow emulate the process used in biological systems. That process appears to be model-based. Rosen provides an explanation for anticipatory behavior of biological systems in terms of interacting models.

Rosen shows that traditional reductionist modeling does not provide simple explanations for complex behavior. What seems to be complex behavior in such models is in fact an artifact of extrapolating the model outside its effective range. Genuine complex behavior must be described by anticipatory modeling. In Rosen's own words: "In particular, complex systems may contain subsystems which act as predictive models of themselves and/or their environments, whose predictions regarding future behaviors can be utilized for modulation of present change of state. Systems of this type act in a truly anticipatory fashion, and possess many novel properties whose properties have never been explored." In other words, genuine complexity is characterized by anticipation.[21]

Rosen defines a formal AS (a mathematical formulation that exhibits anticipatory behavior) as having five attributes. An AS, $S_2$, must contain the model, M, of another system, $S_1$. The AS, $S_2$, must contain a set of observable quantities that can be linked mathematically to $S_1$ and an orthogonal set that cannot. The predictions of the model, M, can cause an observable change in $S_2$. There must be some observable difference in the interaction between $S_1$ and $S_2$ when the model is present and when it is not. Finally, M must be predictive; based on present knowledge, M must change state faster than $S_1$, such that M's changed state constitutes a prediction about $S_1$. The point of this discussion is that intelligent behavior is model-based and in the absence of models, there is no intelligent behavior. More to the point, these models must bear some resemblance to physical reality if the behavior of the intelligent system is to have utility in the real world.[22]

What is the best way to obtain the models required for an AS? The simple answer is to observe reality to a finite extent and then to generalize from the observations. To do so is inherently to add information to the data or to perform an induction. It requires the generation of a likely principle based on incomplete information, and the principle may later be improved in the light of increasing knowledge. Where several possible models might achieve a desired goal, the best choice is driven by the relative economy of different models in reaching the goal.

## 4. BAYESIAN PARAMETER ESTIMATION

How might this be done in practice with noisy data? The most powerful method is Bayesian parameter estimation.[23] Bayesian drops irrelevant parameters without loss of precision in describing relevant parameters. It fully exploits prior knowledge. Most important, the computation of the most probable values of a parameter set incidentally includes the measure of the probability. That is, the calculation produces an estimate of its own goodness. By comparing the goodness of alternative models, the best available description of the underlying reality is obtained. This is the optimal method of obtaining a model from experimental data, or of predicting the occurrence of future events given knowledge from the past, and of improving the prediction of the future as knowledge of the past improves.[24] Bayesian parameter estimation is a straightforward method of induction.

Bayesian parameter estimation describes our best guess of the description of the signal as the weighted sum of several model functions. Its amplitude, or linear parameter, gives the relative contribution of each model function to the overall model. In addition, within each model function, there may be one or more nonlinear parameters. In this technique, the distinguishing feature of a physical effect is the list of model functions and their parameters. This is a somewhat more general concept of the "feature vector" of conventional pattern recognition.

There are as many amplitude parameters as model functions, but the nonlinear parameters in each model function must be searched for. All the nonlinear parameters are included in the argument of the probability function; the amplitude parameters are implicit in the number of model functions in the model (the model's dimensions). The time or sampling points is assumed

to consist of a sequence of regularly spaced integers from 1 to the length of the data set. If we wish to scale the sampling points, simply include the scale factor as a (known) nonlinear parameter. Thus, the model for a single oscillatory term might be

$$\{1, \cos(\omega t), \sin(\omega t)\} \text{ or } \{1, \cos(2\pi\omega t\kappa), \sin(2\pi\omega t\kappa)\} \quad (2)$$

where $\kappa$ is a scaling factor that takes the integer samples represented by t to microseconds, for example, letting $\omega$ represent the frequency in MHz. In the first expression, $\omega$ is the frequency in radians. Consider a model of linear chirp:

$$\{1, \cos(2\pi\omega t\kappa + \alpha\kappa^2 t^2), \sin(2\pi\omega t\kappa + \alpha\kappa^2 t^2)\}. \quad (3)$$

Here, there are three explicit nonlinear parameters ($\alpha$, $\kappa$, and $\omega$) and three implicit amplitude parameters. One of the nonlinear parameters is known, namely $\kappa$, the time-scale parameter. The two unknown parameters are $\alpha$ and $\omega$, leading to a two-dimensional search or optimization problem in the $\omega$, $\alpha$-plane. Generally, if there are m unknown nonlinear parameters, the problem becomes a search in an m-dimensional space for the peak of the likelihood function. Should this prove too much of a computational burden, individual nonlinear parameters may be removed by integration in the usual manner—however, this may prove more difficult than a high-dimensional search.

Log likelihood is the log of the Student-t distribution. This assumes an integration over all the linear model parameters. The Student-t is computed from the projection of the data onto the orthogonalized model—which should be the same number as the projection of the data onto the model and the inner product of the data vector with itself as $S_t = [1 - (d.m/d.d)]^{(m-n)/2}$, where d.m is the projection of the data onto the model and d.d is the projection of the data onto itself.

## 5. EXPERIMENTAL RESULTS

The observables measured in this experiment are the broadband AE signatures of a venturi chamber. Neill et al. found these AE data contain features of incipient cavitation and may contain features of impending cavitation.[25] They used a system that worked nominally through 1.25 MHz but the AE sensor response rolled off substantially above 80 kHz. Therefore, useful information at the high frequency end was lost. They reported unmistakable features of incipient cavitation and concluded that much richer information was being lost due to the limitations of the then-available hardware.

To search for features of impending and incipient cavitation in AE data, the experiment reported in this paper began where the work of Neill et al. left off. The authors used a flow loop at Oak Ridge National Laboratory (ORNL) that is routinely used for calibrating various flow devices. The source of AE signatures was a venturi chamber inserted into the flow loop. The venturi chamber was designed specifically for this experiment and is similar to the one described by Neill et al.

The authors used a Vallen Systeme AMSY4-MC6 AE monitor (Vallen ID number 40900) to collect the data. A complete set of AE signatures at various flow rates was collected with broadband piezo-electric AE sensors (Vallen SE-1025-H, usable frequency response from 10 kHz through greater than 400 kHz). Another complete set of AE signatures at various flow rates was collected with narrowband piezo-electric AE sensors (Vallen SE-9125-M, usable frequency response from 20 kHz through 200 kHz). Sampling rate was 10 million samples per second. Dynamic range was approximately 80 dB. This paper includes highlights from the experimental data. A more exhaustive report of the data will be compiled in a report at ORNL to be published at a future date.

A typical example of the time-domain signature of a cavitation event seen in the AE data is shown in Figure 1. This type of signature occurs very frequently at high flow rates (thousands of instances per second at flow rates above 20 gallons per minute (gpm)). This is a particularly clean instance from the unrefined raw data of the many cavitation events observed at 30 gpm and is used to derive a model of the cavitation event. The amplitude is normalized to 1 at the peak value of the signature. The time-axis is in units of $\mu$sec.

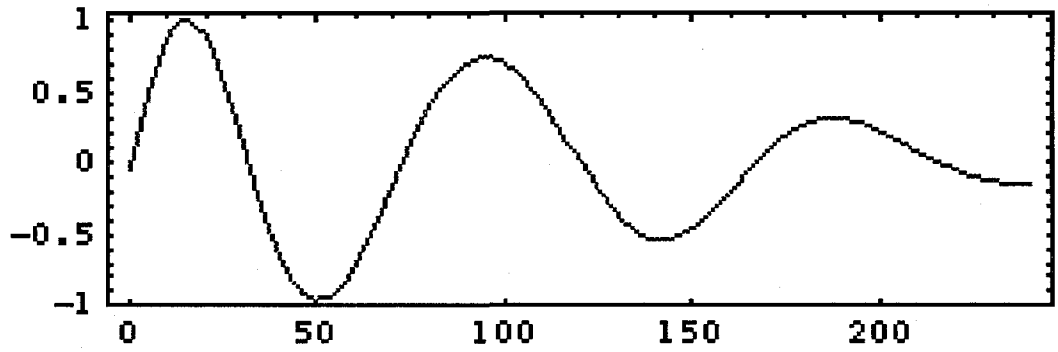


Figure 1. AE signature at 30 gpm.

A linear-chirped damped sinusoid is easily fitted to these data. The model is $\{e^{-\gamma t}\cos(\omega t\kappa + \alpha\kappa^2 t^2), e^{-\gamma t}\sin(\omega t\kappa + \alpha\kappa^2 t^2)\}$. Assume $\kappa$=1. Bayesian parameter estimation computes that the most probable nonlinear parameter values are $\omega$ = 0.0877091, $\alpha$ = -0.000923205, and $\gamma$ = 0.00553404. As shown in Figure 2, this provides a very good first order fit to the data. The damped chirp model is used in the subsequent analyses in this paper. The utility of a more sophisticated model (nonlinear chirps and other decay envelopes) to describe these data will be investigated in future research.

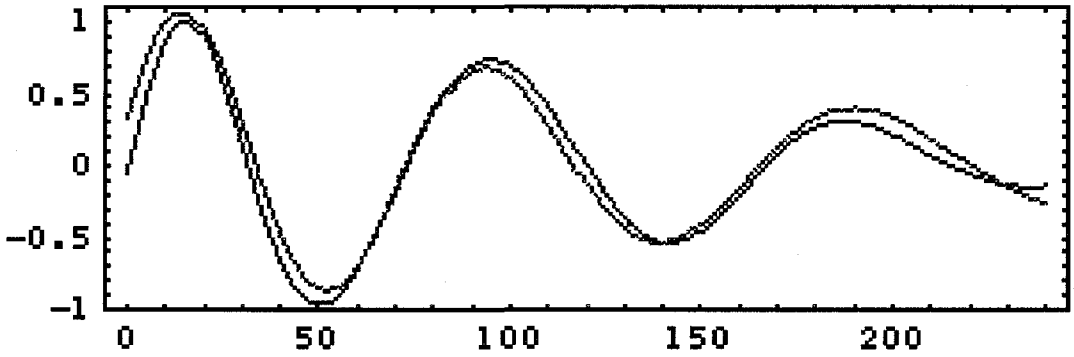


Figure 2. Fitted damped chirp model and observed data.

A typical frame of data captured at 30 gpm with the narrowband sensor is shown in Figure 3. From the audible crackling from the venturi chamber, we know that severe cavitation was occurring. Figure 3 shows a little over 2000 μsec of data with maximum amplitude of approximately 20,000 μV.

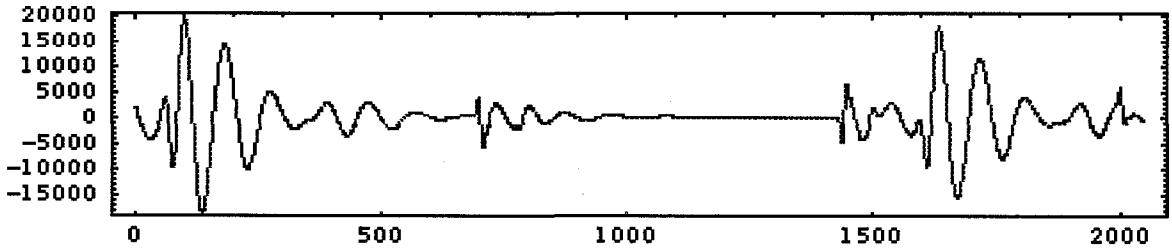


Figure 3. Several cavitation events at 30 gpm.

Likelihood is computed for each set of 240 data points in the signature data while the model (used as a matched filter) is swept forward one sample at a time. The nonlinear parameters and then the linear parameters are calculated for the model and

the goodness of the fit is determined by computing the log (likelihood) in dB. As shown in Figure 4, the signature of Figure 3 includes four events that are very likely damped chirp events. Similar data are shown in Figures 5 and 6 at a 20 gpm flow rate.

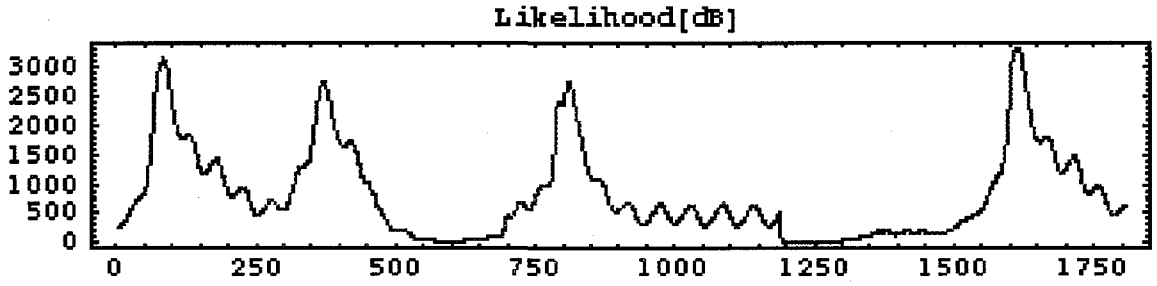


Figure 4. Likelihood of damped chirp events in the signature in Figure 3.

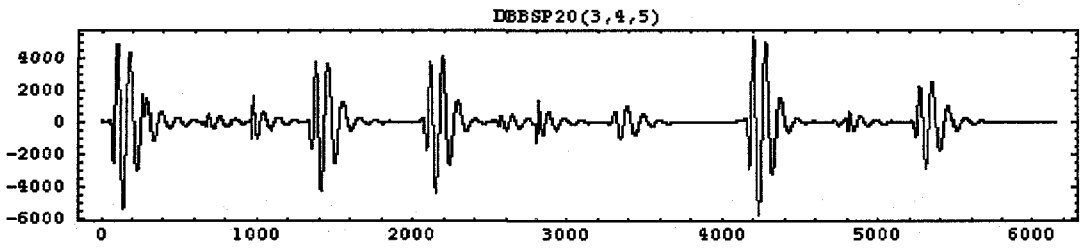


Figure 5. Several cavitation events at 20 gpm.

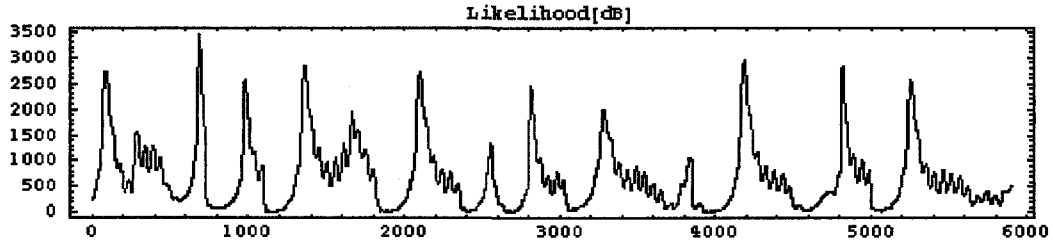


Figure 6. Likelihood of damped chirp events in the signature in Figure 5.

At flow rates below 18 gpm, damped chirp features are very rare occurrences. As Figures 7 and 8 show, a typical data set collected at 17 gpm is practically indistinguishable from the electronic noise of the experimental setup. [Note: The noise floor of the electronics is 1 μV rms. The vertical axis of Figures 3, 5, 7, and 9 is raw sensor output in μV.]

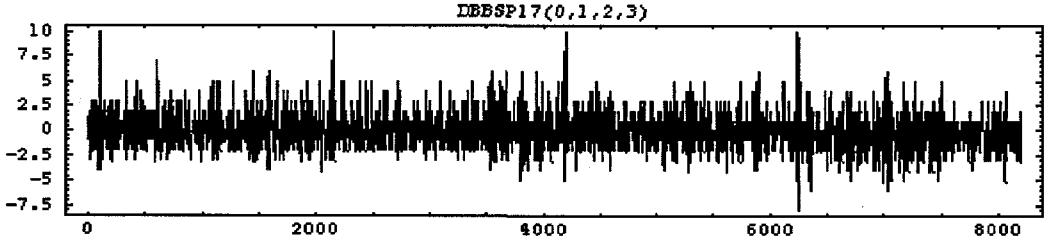


Figure 7. Typical data set at 17 gpm.

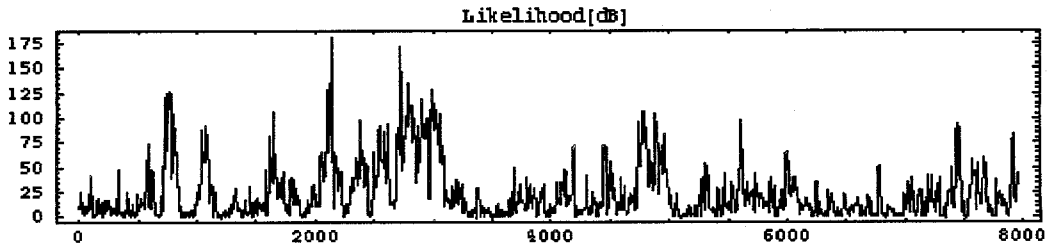


Figure 8. Likelihood of damped chirp events in the signature in Figure 7.

Compare Figures 7 and 8 with Figures 9 and 10. Figure 9 is a typical time domain signature with the sensors mounted on the venturi section but with zero flow through the flow loop. This is the AE signature of the noise from the environment plus the experimental apparatus itself. As seen in Figure 10, if the log likelihood measure is below 750, it is very unlikely that a damped chirp feature is present in the data.

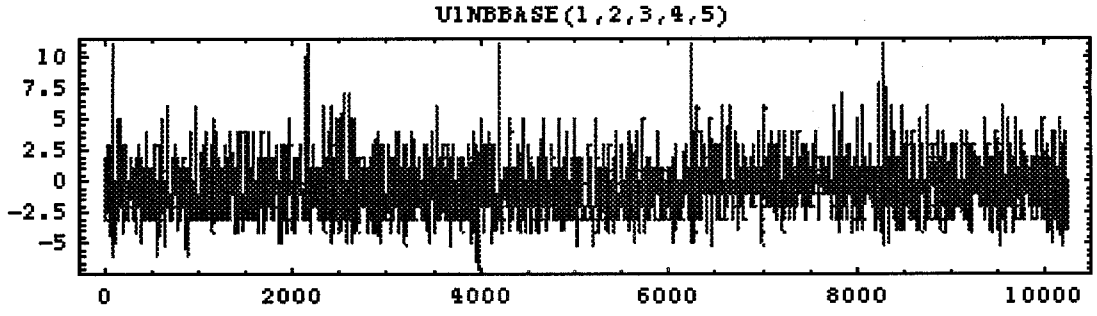


Figure 9. Typical data set at zero flow.

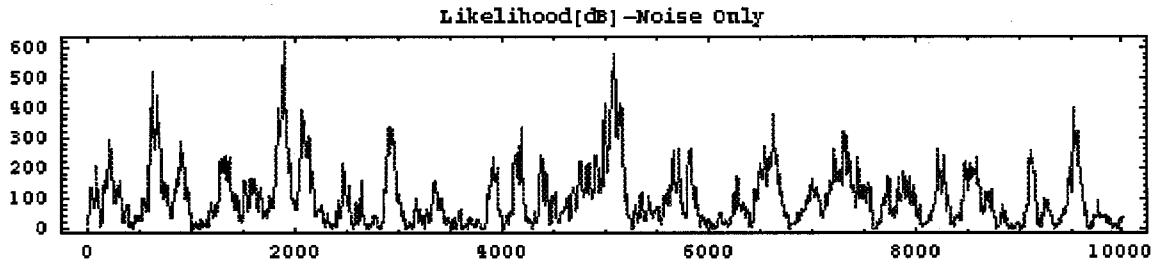


Figure 10. Likelihood of damped chirp events in the signature in Figure 9.

Although damped chirps are rare at 17 gpm, they do occur occasionally. Figure 11 (time domain shown higher, likelihood shown lower) shows the only event captured at 17 gpm with the broadband sensors that do not look just like noise. Two bursts are apparent in the time domain data—a stronger burst near the beginning and a weaker one just after the strong one. Both are only a little stronger than the background noise.

Figure 12 shows more details of the log likelihood plot from Figure 11. It is noteworthy that the weaker burst between times 700 and 900 is more likely to be a damped chirp than the stronger burst between times 200 and 400. If the "threshold of cavitation" is between 17 and 18 gpm, it is possible that the very weak damped chirp (amplitude on the order of 10 $\mu$V) in the 17 gpm data is a precursor to the very strong damped chirp (amplitude on the order of 10 mV) signature in the data at 18 gpm and above. This will be investigated in more detail in future research.

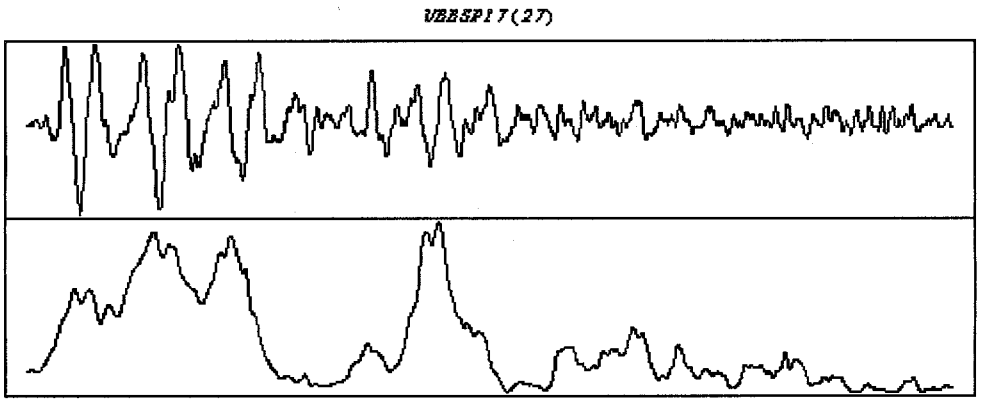


Figure 11. A possible damped chirp at 17 gpm.

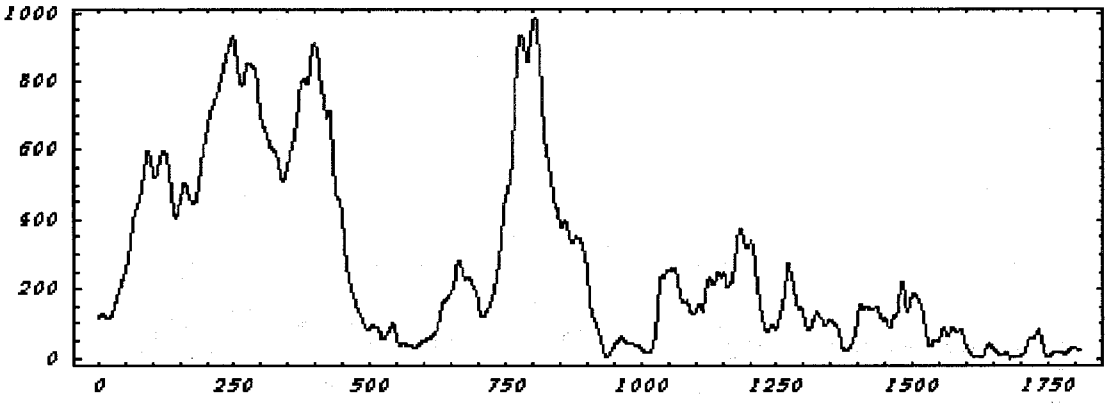


Figure 12. Log likelihood of damped chirp at 17 gpm.

Comparing the 17 gpm data with the zero flow data, it appears that a crude way to distinguish between the presence and absence of damped chirps is to use the log likelihood of 750 as a threshold. The damped chirp appears to be a cavitation signature, although this remains to be confirmed by further investigation. Weak damped chirps (amplitudes of approximately 10 $\mu$V with this experimental setup) with a high log likelihood (greater than 750) appear to be a useful cavitation precursor.

In future work, a less crude (and more reliable) method of deciding whether or not the cavitation signature is present would be a Rosen anticipation engine. The interacting models in the Rosen anticipation engine would be derived from experimental data similar to these and the theory already described. Such a system would inductively learn the signature of cavitation, with the effectiveness of the learning improving over time as the anticipation engine gains experience.

A bit of interpretation of the data yields some useful guidance at this point. The dominant frequencies of the damped chirps are in the digital frequency range of $0.08 <= \omega <= 0.1$ radians. The sampling rate is $10^7$ samples per second, meaning that the digital frequency of $\pi$ corresponds to 5 MHz. Thus, the underlying dominant frequency of the physical chirps is in the range of 127-159 kHz. This is well within the flat response range of the broadband AE sensors. It is also in the resonance peak of the narrowband sensors whose sensitivity in the resonant band tends to be 5-15 dB greater than the sensitivity of the broadband sensors. This suggests that at flow rates below 17 gpm, we should see occasional weak high-likelihood damped chirps with the narrowband sensors. We did.

For example, consider the data set shown in Figure 13, observed at 14 gpm with the narrowband sensors. Note that the two bursts most likely to be damped chirps are barely stronger than the noise and that the matched filter does not show a strong response to the much stronger signal that is unlikely to be a damped chirp.

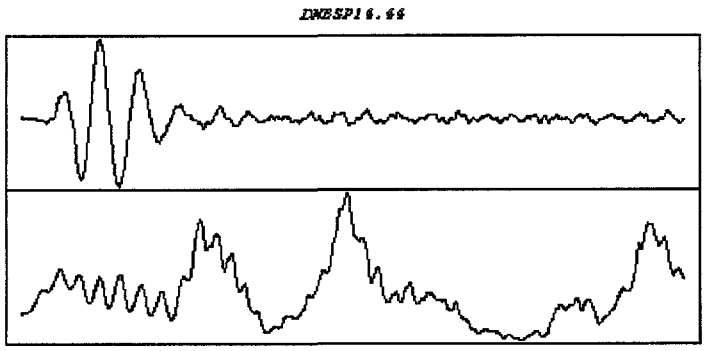

Figure 13. Likely damped chirps at 14 gpm in narrowband data.

Figure 14 shows more details of the log likelihood plot. It is noteworthy that three very weak damped chirps (amplitude below 10 μV) in the 14 gpm data are very likely to be damped chirps. It is also noteworthy that the strong burst at the beginning of the time domain signal is unlikely to be a damped chirp. Among other things, this illustrates that Bayesian parameter estimation does not confuse strong undesired signals with the damped chirp. Similar results are seen at 13 gpm, but the events are rarer and weaker than at higher flow rates.

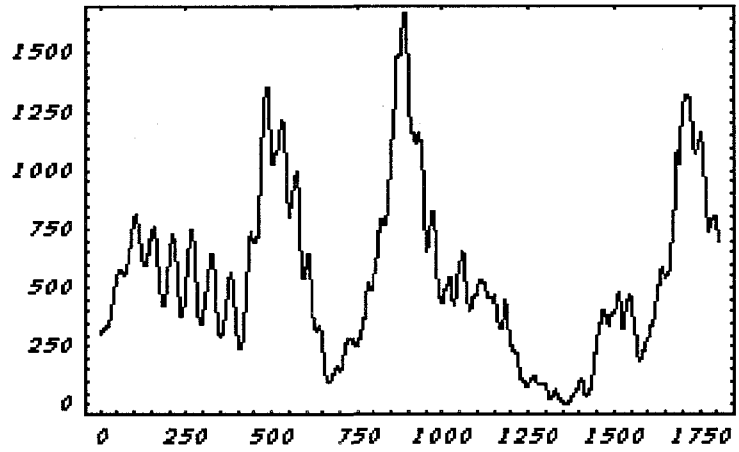


Figure 14. Log likelihood of damped chirps at 14 gpm.

## 6. CONCLUSIONS AND FURTHER RESEARCH

The foregoing analysis is very preliminary and needs to be validated both by further analysis of the extensive data collected during the initial phase of this research and by the collection of additional data. However, several preliminary conclusions appear to be reasonable. First, that damped chirp AE signature seems to be a distinguishing feature of cavitation. Second, above the "threshold of cavitation" strong damped chirps are common occurrences. Third, below the "threshold of cavitation" weak damped chirps are rare (but not non-existent) occurrences. Fourth, the amplitude of the damped chirps drops abruptly at the "threshold of cavitation," consistent with the concept that the inception of cavitation is a catastrophic bifurcation. Fifth, damped chirps are easy to detect and hard to confuse with other signatures when Bayesian parameter estimation is used. Sixth, at flow rates well below the threshold of cavitation, occasional damped chirps are observed with weak amplitudes (virtually indistinguishable from noise by the eye), but with high log likelihood measure.

These conclusions have utility in two aspects of cavitation detection. First, it appears that the sudden emergence of strong damped chirps in response to a small increase in flow rate is a strong and reliable indicator of the inception of cavitation. Second, weak damped chirps at low flow rates appear to be cavitation precursors. This suggests that the Bayesian-derived

damped chirp may be well suited to be a model in the anticipation engine in a formal Rosen AS. These data and their Bayesian analysis illustrate the principle that Rosen's formalism can be used on real-world data to anticipate catastrophic occurrences.

## ACKNOWLEDGMENTS

This research was a joint research effort with AEPTEC Microsystems, Inc., and supported under their SBIR No. N98-114.

## REFERENCES

[1] Christopher E. Brennen, *Hydrodynamics of Pumps*, pp. 74-76, Oxford University Press, Oxford, 1994.
[2] Ibid., p. 78.
[3] Christopher E. Brennen, *Cavitation and Bubble Dynamics*, pp. 34-37, Oxford University Press, Oxford, 1995.
[4] Ibid., pp. 43-48.
[5] Brennen, *Hydrodynamics*, pp. 99-104.
[6] Brennen, *Cavitation*, pp. 79-80.
[7] Brennen, *Hydrodynamics*, pp. 108-111.
[8] Ibid., pp. 111-118.
[9] S. Kumar and C. E. Brennen, "Some Non-Linear Interactive Effects in Bubbly Cavitation Clouds," *Journal of Fluid Mechanics*, Vol. 253, pp. 565-591, 1993.
[10] Brennen, *Cavitation*, pp. 83-91.
[11] Ibid., pp. 182-187.
[12] Ibid., pp. 188-193.
[13] Ibid., pp. 193-201.
[14] Ibid., pp. 194-201.
[15] S. W. Kercel, "Peering Through A Dirty Window: A Bayesian Approach to Making Mine Detection Decisions From Noisy Data," *IEEE International Conference on Systems, Man, and Cybernetics*, LaJolla, CA, October 14, 1998.
[16] C. Landauer and K. L. Bellman, "Semiotics of Constructed Complex Systems," in *Intelligent Systems: A Semiotic Perspective*, J. Albus, A. Meystel, and R. Quintero, Organizers, pp. 35-40, National Institute of Standards and Technology, Gaithersburg, MD, 1996.
[17] C. Landauer, "Constructing Autonomous Software Systems," *Workshop on Biologically Inspired Autonomous Systems: Computation, Cognition, and Action*, Durham, NC, March 4-5, 1996.
[18] K. L. Bellman, "When Intelligence is in Control," in *Intelligent Systems: A Semiotic Perspective*, J. Albus, A. Meystel, and R. Quintero, Organizers, pp. 10-11, National Institute of Standards and Technology, Gaithersburg, MD, 1996.
[19] L. Goldfarb and S. Nigam, "The Unified Learning Paradigm: A Foundation for AI," in *Artificial Intelligence and Neural Networks: Steps Toward Principled Integration*, V. Honovar and L. Uhr, Editors, Academic Press, Boston, 1994.
[20] L. Goldfarb, "Inductive class representation and its central role in pattern recognition," in *Intelligent Systems: A Semiotic Perspective*, J. Albus, A. Meystel, and R. Quintero, Organizers, pp. 53-58, National Institute of Standards and Technology, Gaithersburg, MD, 1996.
[21] R. Rosen, "Some Epistemological Issues in Physics and Biology," in *Quantum Implications Essays in Honour of David Bohm*, Edited by B. J. Hiley and F. D. Peat, Routledge and Kegan Paul, London, pp. 314-327, 1987.
[22] R. Rosen, *Anticipatory Systems: Philosophical, Mathematical, and Methodological Foundations*, Pergammon Press, Oxford, 1985.
[23] L. Bretthorst, *Bayesian Spectrum Analysis and Parameter Estimation*, pp. 1-5, Springer-Verlag, Berlin, 1988.
[24] E. T. Jaynes, "Generalized Scattering," in *Maximum-Entropy and Bayesian Methods in Inverse Problems*, C. R Smith and W. T. Grandy, Editors, pp. 377-398, D. Reidel Publishing Co., Holland, 1985.
[25] G. D. Neill, R. L. Reuben, P. M. Sanford, E. R. Brown, and J. A. Steel, "Detection of incipient cavitation in pumps using acoustic emission," *Proceedings of the Institution of Mechanical Engineers*, Part E, Vol. 211, pp. 267-277, 1997.